Supplemental Material for "Thermalization Universality-Class Transition Induced by Anderson Localization"

Weihua Zhang,[1,2] Gabriel M. Lando,[1] Barbara Dietz,[1] and Sergej Flach[1]

[1] *Center for Theoretical Physics of Complex Systems, Institute for Basic Science, Daejeon 34126, Republic of Korea*

[2] *Lanzhou Center for Theoretical Physics and the Gansu Provincial Key Laboratory of Theoretical Physics, Lanzhou University, Lanzhou, Gansu 730000, China*

This supplementary material complements the main text by providing additional information on the numerical procedures that were employed to compute Lyapunov spectra. It includes a comprehensive description of the dynamic evolution of the unitary circuits maps used in our simulations. Additionally, we outline the specific initial conditions adopted for the simulations and elaborate on the convergence criteria applied for obtaining the Lyapunov spectrum (LS).

I. DYNAMIC EVOLUTION

For the sake of simplicity, we use the notation $\{\psi_{2n}(t), \psi_{2n+1}(t)\}^T$ to represent the states of two sites within a single unit cell (depicted as violet and brown circles in Fig. 1 of the main text). The time evolution of these states is governed by the equations [1, 2]:

$$\psi_n(t+1) = e^{i\epsilon_n} e^{i(g|f_n[\vec{\Psi}(t)]|^2)} f_n[\vec{\Psi}(t)], \tag{S1}$$

$$\tag{S2}$$

with

$$\begin{aligned} f_{2n}[\vec{\Psi}(t)] &= \mathcal{C}^2\psi_{2n}(t) - \mathcal{C}\mathcal{S}\psi_{2n-1}(t) + \mathcal{S}^2\psi_{2n-2}(t) + \mathcal{C}\mathcal{S}\psi_{2n+1}(t), \\ f_{2n-1}[\vec{\Psi}(t)] &= \mathcal{C}^2\psi_{2n-1}(t) - \mathcal{C}\mathcal{S}\psi_{2n-2}(t) + \mathcal{S}^2\psi_{2n+1}(t) + \mathcal{C}\mathcal{S}\psi_{2n}(t), \end{aligned} \tag{S3}$$

where $\mathcal{C} = \cos\theta$ and $\mathcal{S} = \sin\theta$.

II. INITIAL CONDITIONS

In all simulations, we initialize the system with initial conditions $|\psi_n|e^{i\phi_n}$, $n = 1, 2, \ldots N$ for the nth component of $\vec{\Psi}(0)$, where the phases ϕ_n are uncorrelated and uniformly randomly distributed in the range $[-\pi, \pi]$, and the rescaled squared amplitudes $\eta_n = N|\psi_n|^2$ follow an exponential distribution $p(\eta) \propto e^{-\eta/\langle\eta\rangle}$. The average value of the square-norm of ψ_n is normalized to $\langle\eta\rangle = \frac{1}{2}$ which is consistent with the approach used in Refs. [1, 2].

The strengths of disorder, denoted by ϵ_n, are also uncorrelated and uniformly randomly distributed in the interval $[-\pi, \pi]$, following the procedure described in Ref. [3].

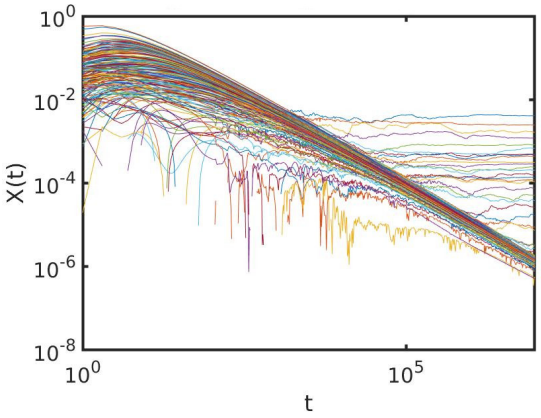

FIG. S1. Evolution of positive transient LS with $\theta = 0.00075$ and $g = 1$. $N = 100$, $T_s = 10^7$.

III. LYAPUNOV SPECTRUM CALCULATION

The Lyapunov exponent measures the exponential growth rate of an infinitesimal distance $w(t)$ from the initial trajectory. It is defined as $\Lambda = \lim_{t\to\infty} \frac{1}{t} \ln \frac{w(t)}{w(0)}$ [4]. To compute the positive LS, we introduce N orthogonal perturbations $\vec{w}(t)$ to trajectories $\vec{x}(t)$, where N is equal to the degree of freedom of the system and the state $\vec{\Psi}(t) = \vec{x}(t) + \vec{w}(t)$ follows the equations of motion Eq. (S1).

Because of the linearity property $f_n[\vec{\Psi}(t)] = f_n[\vec{x}(t)] + f_n[\vec{w}(t)]$, we can expand the norm in the exponential term in Eq. (S1). We only keep the first order of $\vec{w}$,

$$\begin{aligned} &|f_n[\vec{\Psi}(t)]|^2 = |f_n[\vec{x}(t)] + f_n[\vec{w}(t)]|^2 \\ &= |f_n[\vec{x}(t)]|^2 + |f_n[\vec{w}(t)]|^2 + 2\,\mathrm{Re}\{f_n[\vec{w}(t)]f_n[\vec{x}(t)]^*\} \\ &\approx |f_n[\vec{x}(t)]|^2 + \mathrm{Re}_n \end{aligned}$$

where $\mathrm{Re}_n = 2\,\mathrm{Re}\{f_n[\vec{w}(t)]f_n[\vec{x}(t)]^*\}$.

Expanding the nonlinear part in a Taylor series and retaining only the first order of $\vec{w}(t)$, we obtain

$$\begin{aligned} e^{ig|f_n[\vec{\Psi}(t)]|^2} &= e^{i|f_n[\vec{x}(t)]|^2} e^{ig\,\mathrm{Re}_n} \\ &\approx e^{i|f_n[\vec{x}(t)]|^2}(1 + ig\,\mathrm{Re}_n). \end{aligned}$$

Subtracting the contribution from the linear trajectories

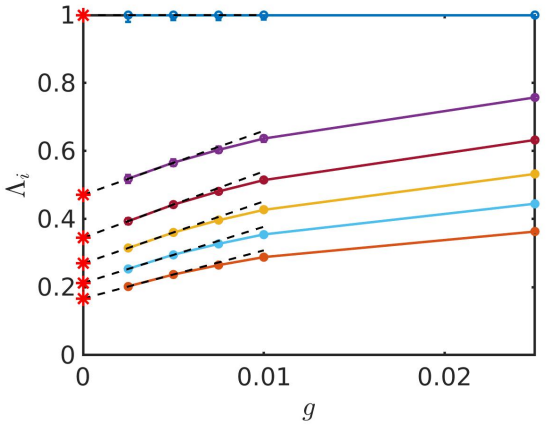

FIG. S2. The colored lines show Λ_i versus g. The black dashed lines show the extrapolation process. The red stars show the points that are used in the plots of the asymptotic curves.

yields the growth of the perturbation

$$w_n(t+1) = \psi_n(t+1) - x_n(t+1)$$
$$= e^{i\epsilon_n} e^{i(g|f_n[\vec{x}(t)]|^2)} \{f_n[\vec{w}(t)] + ig\,\mathrm{Re}_n\, f_n[\vec{x}(t)]\}.$$

Fig. S1 exemplifies the evolution of the positive transient LS for one specific case.

IV. SATURATION CRITERION AND ASYMPTOTIC CURVE OF RESCALED LYAPUNOV SPECTRUM

A. Saturation criterion of Lyapunov spectrum

As we approach an integrable limit, the divergent timescales become inversely proportional to the LS. However, due to computational limitations, we are required to terminate our evolution at a specific number of time steps, typically ranging from 10^8 to 10^9 in this study. Despite this limitation, even at these time steps, certain parts of the LS may not have reached saturation. To quantify the saturation level, we calculate the standard deviation σ_t of the data between the final time, 10^{n_s}, and its previous "generation", 10^{n_s-1}. This interval typically covers more than 90% of the total evolution time.

To control the accuracy of our simulations, we utilize the parameter $L = \frac{\sigma_t}{\Lambda_{\max}}$, where $\Lambda_{\max}$ is the maximum Lyapunov exponent. We found out that the requirement $L \leq L_{max} = 0.11$ is sufficient to obtain reliable results for the Lyapunov exponents Λ_i.

B. Asymptotic curve of rescaled Lyapunov spectrum

Fig. S2 depicts the extrapolation process used to obtain the results plotted in Fig. 5 of the main text. The values of the smallest and second smallest perturbation strength g were determined based on the required accuracy $L \leq L_{max}$. To obtain information on the Λ_i when g approaches zero, we perform linear extrapolation of these two points. The red stars in Fig. S2 exemplary indicate the values of the Lyapunov exponents (LEs) that are used in the plots of asymptotic curves resulting from such an extrapolation procedure. These LEs capture the behavior of the system as g approaches zero and provide valuable insights into the system properties in the near-integrable regime.

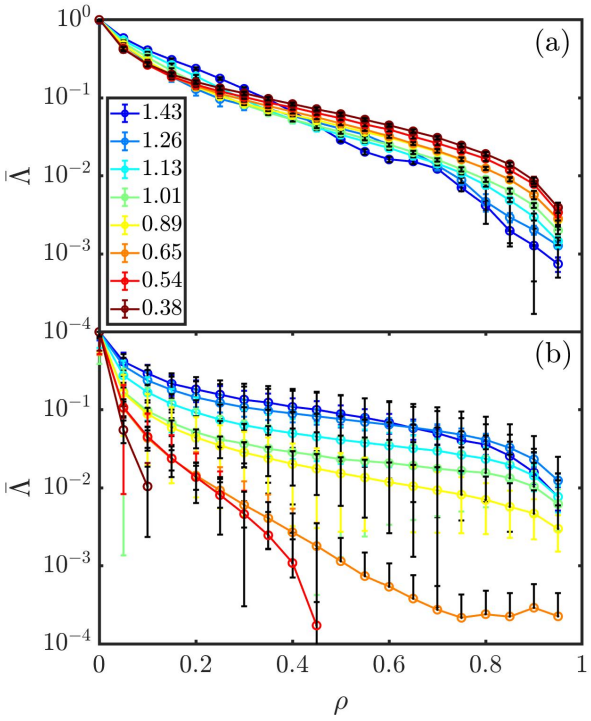

FIG. S3. Asymptotic curves for rescaled LS versus rescaled index ρ for the (a) ordered cases and (b) disordered cases in log scale. The angle θ varies from 1.43 (blue) to 0.38 (red). The error bars represent the time (σ_t black) and ensemble (σ_g colored) standard deviations. For all cases, the system size is $N = 200$. Unphysical error bars that would generate negative exponents are removed in panel (b).

Using this extrapolation procedure, we have obtained the asymptotic curves for the rescaled Lyapunov spectra of both ordered and disordered cases, considering different values of θ. These curves are depicted in Fig. S3. The rescaled Lyapunov spectra provide valuable insights into the thermalization universality-class transition induced by disorder and the impact of localization on the system's behavior in the near-integrable regime.

V. FITTING OF LYAPUNOV SPECTRUM

To further illustrate the distinct characteristics of the short- and long-range networks, we employ Eq. (5) from

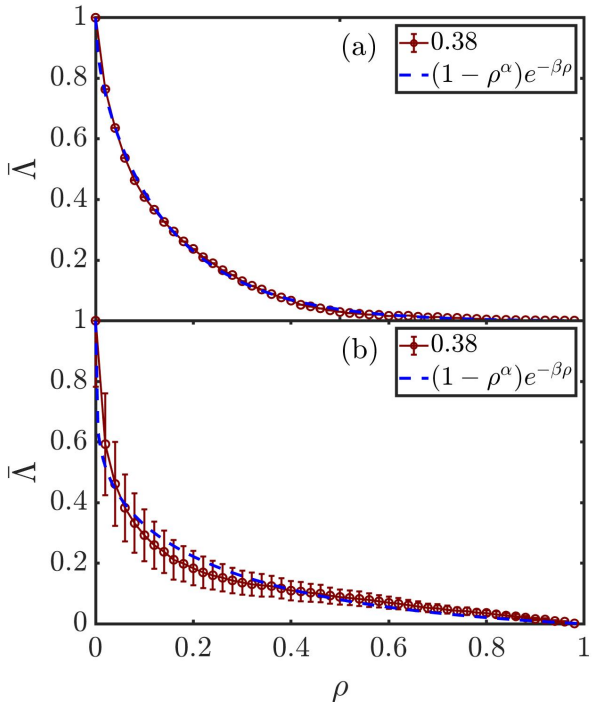

FIG. S4. Asymptotic curves (red) for the rescaled LS versus rescaled index ρ for the (a) ordered and (b) disordered cases in log scale. The angle θ is equal to 0.38. The error bars represent the ensemble (σ_g) standard deviations. The blue dashed curves are the fittings.

the main text to fit the rescaled LS.

Fig. S4 presents one example for the fit of the proposed ansatz Eq. (5) of the main text to the rescaled LS for the ordered case and one for the disordered case. This fitting procedure allows us to better understand the behavior of the system and the underlying thermalization universality-class transition induced by Anderson localization. The fitted curves provide valuable insights into the relationship between the localization length ξ and the thermalization behavior in the near-integrable regime.

VI. FIT COEFFICIENT α FOR ASYMPTOTIC CURVES OF ORDERED AND DISORDERED UNITARY CIRCUITS MAPS

Fig. S5 displays the fit coefficients α obtained from Eq. (5) of the main text as a function of θ for the asymptotic curves shown in Fig. S3. In the plot, the red triangles connected by red dashed lines represent the fit coefficients for ordered systems, while the blue triangles connected by blue straight lines represent the fit coefficients for disordered systems.

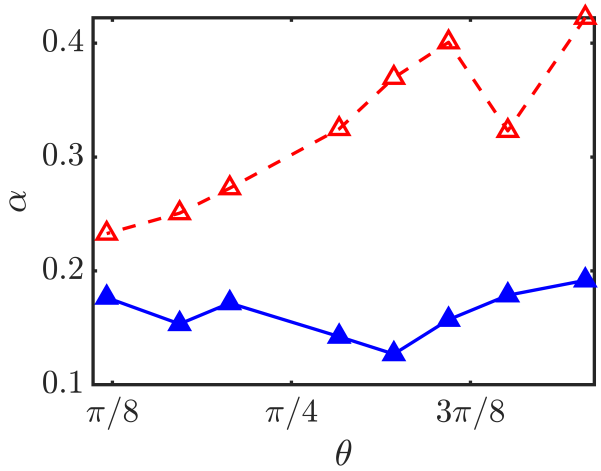

FIG. S5. Fit coefficient α (β is shown in Fig. 5 of the main text) of Eq. (5) in the main text versus θ for the asymptotic curves of the ordered (red empty triangles) and disordered (blue filled triangles) unitary circuits maps.

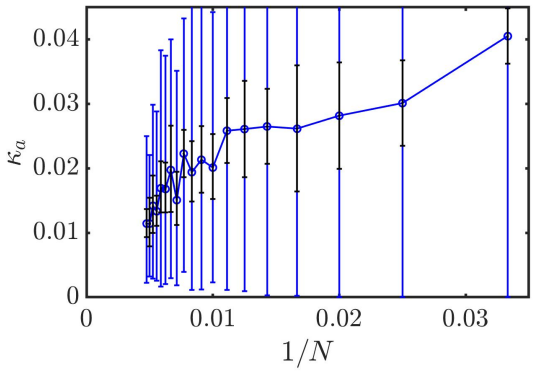

FIG. S6. κ_a versus $1/N$ with localization length $\xi = 2$ ($\theta = 0.65$) for disordered unitary circuits maps. The error bars represent the time (σ_t black) and ensemble (σ_g blue) standard deviations. The number of trajectories is 100.

VII. VARIATION OF κ_a WITH DIFFERENT SYSTEM SIZES

In addition to inducing the transition from a long-range network to a short-range network by varying the localization length ξ, we can also achieve this transition by increasing the system size N. We have calculated the quantity κ_a for different system sizes, all with the same localization length $\xi = 2$, as presented in Fig. S6.

We observe that as the system size N increases, κ_a decreases, providing further evidence for the long- to short-range network transition. Notably, the error bars deduced from ensemble averages are of comparable magnitude to the average value. This observation clearly indicates non-ergodicity and suggests that the maximum achievable time $T_s = 10^8$ may not be sufficient for ergodization in the system. Note also that the ergodization

time diverges much more rapidly in the short-range network regime [5, 6], which will be explored in forthcoming works.

[1] M. Malishava and S. Flach, Lyapunov Spectrum Scaling for Classical Many-Body Dynamics Close to Integrability, Phys. Rev. Lett. **128**, 134102 (2022).

[2] M. Malishava and S. Flach, Thermalization dynamics of macroscopic weakly nonintegrable maps, Chaos **32**, 063113 (2022).

[3] I. Vakulchyk and S. Flach, Universal Anderson localization in one-dimensional unitary maps, Chaos: An Interdisciplinary Journal of Nonlinear Science **33**, 083134 (2023).

[4] C. Skokos, The Lyapunov Characteristic Exponents and Their Computation, in *Dynamics of Small Solar System Bodies and Exoplanets*, Lecture Notes in Physics, edited by J. J. Souchay and R. Dvorak (Springer, Berlin, Heidelberg, 2010) pp. 63–135.

[5] C. Danieli, T. Mithun, Y. Kati, D. K. Campbell, and S. Flach, Dynamical glass in weakly nonintegrable Klein-Gordon chains, Phys. Rev. E **100**, 032217 (2019).

[6] T. Mithun, C. Danieli, Y. Kati, and S. Flach, Dynamical Glass and Ergodization Times in Classical Josephson Junction Chains, Phys. Rev. Lett. **122**, 054102 (2019).